Metrol. Meas. Syst., Vol. 29 (2022) No. 4, pp. 751–762
DOI: 10.24425/mms.2022.143063

PAN POLSKA AKADEMIA NAUK

METROLOGY AND MEASUREMENT SYSTEMS
Index 330930, ISSN 0860-8229
www.metrology.wat.edu.pl

M&MS

A NOVEL BASE STRAIN SENSITIVITY MEASUREMENT SYSTEM WITH STEADY HARMONIC EXCITATION

Chuwei Ye

The State Key Laboratory of Fluid Power Transmission and Control, Zhejiang Province Key Laboratory of Advanced Manufacturing Technology, Zhejiang University, 310027, Hangzhou, China
(✉ *yechuwei@zju.edu.cn*, +1 517 515 3639)

Abstract

Considering the low accuracy and low efficiency of the traditional calibration method for base strain sensitivity of accelerometers, a novel base strain sensitivity calibration system with steady harmonic excitation is proposed. The required cantilever beam for calibration is driven by an electromagnetic exciter to generate a base strain varying in a steady harmonic pattern. By applying a Wheatstone bridge circuit, the generated strain with low distortion can be measured. The measurement system with a compensation function can automatically calibrate the base strain sensitivity. The amplitude linearity and frequency response characteristics of the base strain sensitivity in two accelerometers are obtained experimentally, and the uncertainty in the results is 2% ($k = 2$).

Keywords: base strain sensitivity, piezoelectric accelerometer, steady harmonic excitation, calibration.

1. Introduction

The accurate measurement of vibrations is becoming increasingly dependent on the measuring characteristics of vibration pick-ups. The piezoelectric type accelerometer is widely used in vibration measurement because of its small size and mass, simple structure, wide bandwidth, easy signal conditioning and high stability [1, 2]. In most cases, the vibration pick-ups are treated as sensors with ideal characteristics whose output is totally excited by the vibration stimulations. In other words, the output signals are assumed as a direct response. However, because of the fabrication and assembly errors [3, 4], adverse environment [5, 6], and improper mounting [7, 8], the response of the vibration pick-ups can contain spurious signals, which are called a spurious response.

To verify the characteristics of vibration pick-ups, systems and methods designed for the calibration of direct responses, including frequency response, phase response and nonlinearity, have been well developed in some countries [1, 9, 10, 12]. However, little attention has been given to the spurious response, which can be evaluated by temperature dependency, transient temperature

Article history: received May 25, 2022; revised June 19, 2022; accepted July 4, 2022; available online September 16, 2022.

sensitivity, transverse vibration sensitivity [13], base strain sensitivity, magnetic sensitivity and sensitivity to mounting torque [14], even if this kind of response could introduce an error signal more than 5% [15–18].

The base strain sensitivity, considered as a spurious response of a piezoelectric rectilinear accelerometer, can reflect the error produced by the pick-up when its base is bending. Indeed, efforts to decrease base strain sensitivity have been made by accelerometer manufacturers by optimizing the inner structures, but the method used to calibrate base strain sensitivity, which is defined with a simple calibration method that requires manual operation with a fixed calibration frequency [19], suffers from low accuracy and low efficiency.

In response to this lack of research, a novel measurement system for base strain sensitivity with harmonic excitation has been developed. The novelty of the system is obvious. Firstly, it can generate the base strain accurately from 50 με to 500 με, measured by strain gauges arranged in a Wheatstone bridge circuit; secondly, the excitation frequency is continuously adjustable from 1 Hz to 6 Hz, making it convenient to obtain the frequency response of the base strain sensitivity; Finally, the whole calibration process can be automatically finished by the software, decreasing the probable errors created by manual interference.

2. Design of the base strain sensitivity measurement system

2.1. Overview

In the process of base strain sensitivity calibration, as shown in Fig. 1, the *sensor under test* (SUT) should be mounted 40 mm from the clamped end of a steel cantilever beam, which has a particular shape with a fixed natural frequency close to 4.5 Hz.

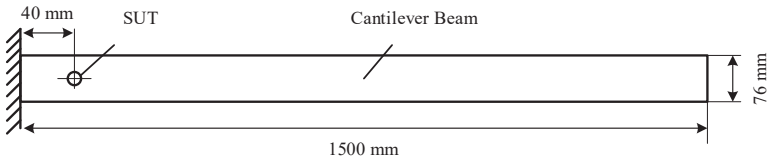

Fig. 1. Model of the cantilever beam used for base strain sensitivity calibration; the thickness is 12.5 mm.

The base strain sensitivity S_ε of the SUT is determined by dividing the maximum output error $a_{\max}$ by the reference strain ε at 250×10^{-6}, with the unit $\mathrm{m{\cdot}s^{-2}/\mu\varepsilon}$, which can be expressed as

$$S_\varepsilon = \frac{a_{\max}}{\varepsilon}. \tag{1}$$

The proposed novel base strain sensitivity measurement system with harmonic excitation is shown in Fig. 2. Fig. 2a illustrates the principal diagram and constitution, and Fig. 2b illustrates the general arrangement of the system. The cantilever beam is suspended vertically with an electromagnetic exciter at the free end, which is driven by a power amplifier providing a steady harmonic current from 1 Hz to 6 Hz to generate an adjustable base strain reaching 500 με for the SUT. The strain is measured by strain gauges in a Wheatstone bridge whose output is transmitted by the circuit conveyor to the controller. The output of the SUT is transmitted to the controller after amplification by the charge amplifier. Bilateral communication between the calibration software and the controller is based on TCP/IP. In addition, a monitor accelerometer is mounted at the free end of the beam, ensuring that the amplitude does not exceed the limitation and aiding to achieve a compensating function, which will be introduced in detail later.

Metrol. Meas. Syst., Vol. 29 (2022), No. 4, pp. 751–762
DOI: 10.24425/mms.2022.143063

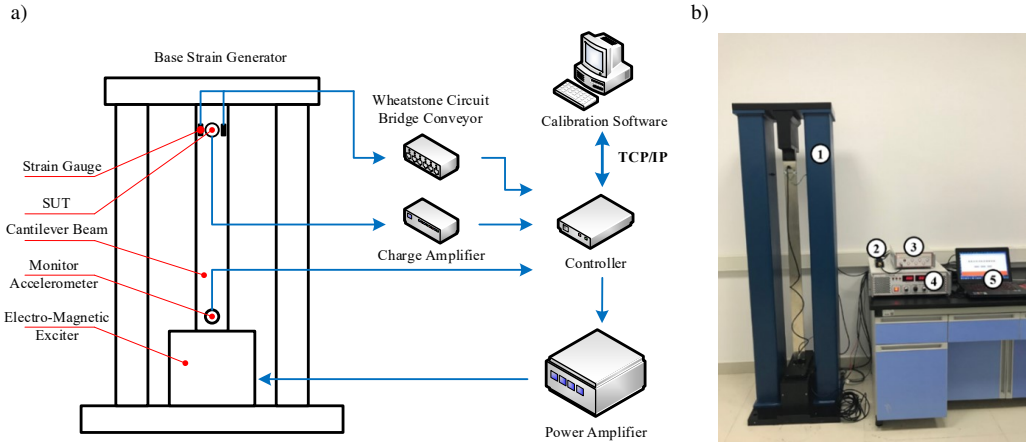

Fig. 2. Principle diagram and constitution of the calibration system (a); Prototype of the calibration system (b).
1. Base strain generator, 2. Wheatstone bridge circuit conveyor, 3. Controller, 4. Power amplifier, 5. Calibration software.

2.2. Design of the base strain generator

A sectional view of the base strain generator is shown in Fig. 3. The generator is divided into a cantilever beam and an electromagnetic exciter circled with a yellow square in dashed lines. Both air gaps a and b in the exciter are filled with uniformly distributed magnetic flux density B, which is produced by the permanent magnets and yokes. A coil is attached to the free end of the beam, conducting sinusoidal current i and offering harmonic excitation. In this way, the strain near the mounting position of the SUT varies sinusoidally.

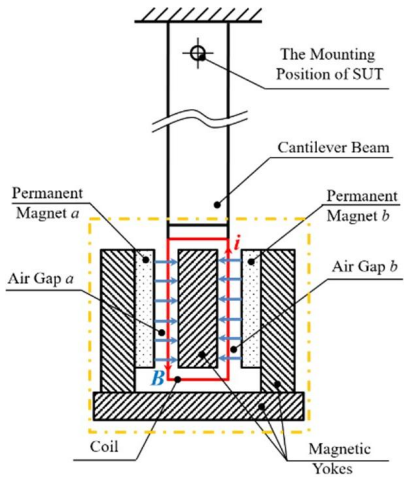

Fig. 3. Structure of the base strain generator (sectional view).

Whether the magnetic flux density is uniformly distributed in both air gaps significantly affects the distortion of the strain waveform in the time domain. In the built prototype, the exact values of the density, which are in 20 separated positions numbered both from 1 to 10 covering both whole air gaps, are measured, and the distribution is illustrated in Fig. 4.

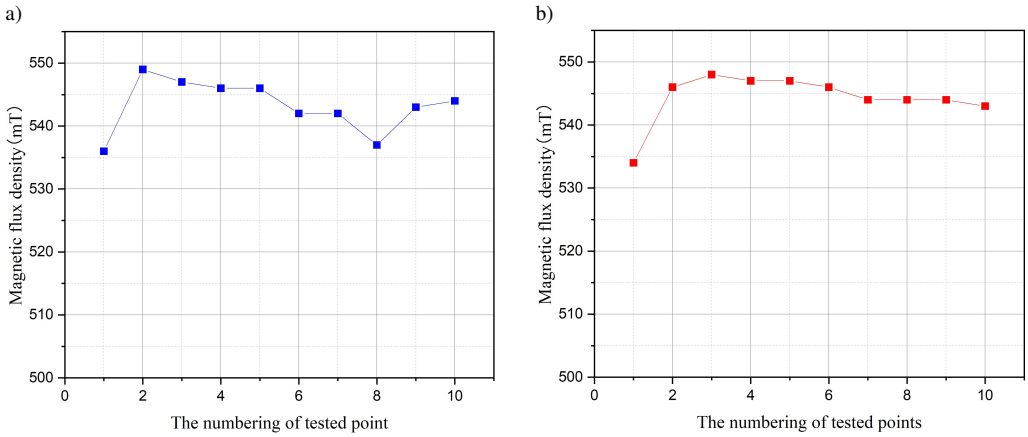

Fig. 4. Distribution of the magnetic flux density in air gaps. Distribution in gap *a* (a); distribution in gap *b* (b).

The uniformity ξ of the magnetic flux density B in each air gap can be calculated as

$$\xi = 1 - \frac{\sqrt{\frac{1}{10}\sum_{i=1}^{10}\left(\bar{B} - B_i\right)^2}}{\bar{B}}, \tag{2}$$

in which $\bar{B}$ is the arithmetical average of the 10 tested points. Therefore, the uniformities in each gap are $\xi_a = \xi_b = 99.3\%$, which absolutely meet the design requirement.

The principle of the coil driving the cantilever beam is relatively easy to understand. When conducting a sinusoidal current, part of the coil in the gaps is subjected to Ampere force. The magnitude of the force F can be calculated as

$$F = Bli, \tag{3}$$

where l is the total length of the coil in the air gaps. To ensure that the Ampere force is sufficient to drive the beam and generate a maximum strain, the length should be appropriate.

2.3. Design of the base strain measurement system with a compensating function

The measurement of the base strain and output of the SUT and the calculation of the base strain sensitivity are included as a function of the measurement system.

First, the base strain is measured by a conventional but reliable Wheatstone bridge circuit, which is shown in Fig. 5. The four identical resistors R_1 to R_4 in the circuit are two pairs of strain gauges, and to measure the base strain each pair is attached to both sides near the SUT but on the opposite surfaces of the beam. To demonstrate in more detail, when strain gauges R_1 and R_3 are compressed, R_2 and R_4 are tensioned with the strain at the same amplitude.

According to the characteristics of the circuit, the following condition is used:

$$R_1 = R_2 = R_3 = R_4 = R. \tag{4}$$

When

$$-\Delta R_1 = \Delta R_2 = -\Delta R_3 = \Delta R_4 = \Delta R \tag{5}$$

Metrol. Meas. Syst., Vol. 29 (2022), No. 4, pp. 751–762
DOI: 10.24425/mms.2022.143063

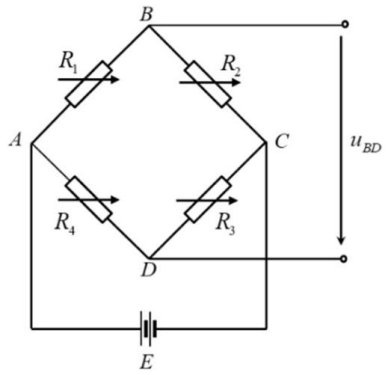

Fig. 5. Wheatstone bridge circuit for base strain measurement.

occurs, which exactly happens to the four strain gauges when the beam is bending, the output variation of the circuit Δu_{BD} can be expressed as

$$\Delta u_{\mathrm{BD}} = E \cdot \frac{\Delta R}{R}, \tag{6}$$

where E is the constant voltage supplied by the DC power. Moreover, in the strain gauges,

$$\frac{\Delta R}{R} = K \cdot \varepsilon, \tag{7}$$

where K is a constant factor and is always satisfied. Therefore, Δu_{BD} can be finally expressed as

$$\Delta u_{\mathrm{BD}} = E \cdot K \cdot \varepsilon. \tag{8}$$

Therefore, when Δu_{BD} is measured in *root mean square* (RMS), the base strain ε can also be calculated in RMS.

Second, the output of the SUT can be measured and displayed by combined action of the charge amplifier, the controller and the calibration software. After compensating against the vibration introduced by the oscillating cantilever beam described in the following section, the base strain sensitivity can be automatically calculated and displayed.

2.4. Compensation method against base vibration

When calibrating the base strain sensitivity, the SUT is expected not to vibrate because the output should be excited by the applied strain only. However, when the free end of the beam oscillates, except for the rigid clamped end, the rest of the beam vibrates, including the position where the SUT is mounted. As a result, the total measured acceleration $a_{\mathrm{total}}(t)$ can be expressed as

$$a_{\mathrm{total}}(t) = a_{\mathrm{base}}(t) + a_{\varepsilon}(t), \tag{9}$$

where a_{ε} is the error output caused by the base strain and $a_{\mathrm{base}}(t)$ is the actual acceleration of the SUT.

To solve this problem, another accelerometer is mounted to serve as a monitor near the free end, as shown in Fig. 6.

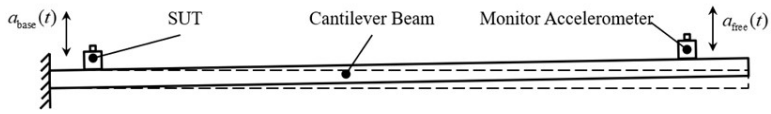

Fig. 6. To compensate for the base vibration, a monitor accelerometer is applied.

When the oscillating amplitude of the free end is small enough compared with the length of the beam, which actually occurs, the relationship is satisfied as

$$k_0 = \frac{a_{\text{base}}(t_i)}{a_{\text{free}}(t_i)}, \tag{10}$$

where k_0 is a constant and $a_{\text{free}}(t)$ is the acceleration of the free end. Index i indicates that the equation is correct at any particular time. Therefore, k_0 can also be expressed as

$$k_0 = \frac{a_{\text{base}\,m}}{a_{\text{free}\,m}}, \tag{11}$$

where the index m indicates the amplitude of the value.

The monitor is an integrated electronics piezoelectric (IEPE)-type sensor whose output is in voltage already converted from charge by its inner circuit. Therefore, $a_{\text{free}\,m}$ can be expressed as

$$a_{\text{free}\,m} = \frac{u_{\text{free}\,m}}{S_{\text{free}}}, \tag{12}$$

where $u_{\text{free}\,m}$ and S_{free} represent the amplitude of the output voltage and sensitivity of the monitor, respectively. Moreover, $a_{\text{base}\,m}$ can be measured by a laser vibrometer.

In conclusion, the error output caused by the base strain can be expressed as

$$a_{\varepsilon}(t) = a_{\text{total}}(t) - a_{\text{base}}(t) = \frac{u_{\text{total}}(t)}{S_{\text{base}}} - \frac{a_{\text{base}\,m}}{u_{\text{free}\,m}} \cdot u_{\text{free}}(t), \tag{13}$$

where u_{total} and S_{base} are the output in voltage and the sensitivity of the SUT, respectively.

The output voltages of each sensor are sampled as point series by the controller, and the RMS of each series can be analyzed by calibration software. The final expression of measured base strain sensitivity is

$$S_{\varepsilon} = \frac{a_{\varepsilon}(t)_{\text{rms}}}{\varepsilon(t)_{\text{rms}}} = E \cdot K \cdot \frac{\left[\frac{u_{\text{total}}(t)}{S_{\text{base}}} - \frac{a_{\text{base}\,m}}{u_{\text{free}\,m}} \cdot u_{\text{free}}(t)\right]_{\text{rms}}}{\Delta u_{\text{BD}}(t)_{\text{rms}}}, \tag{14}$$

where the index rms represents the value in RMS.

3. Experimental results

3.1. The waveform results

The strain generated by the generator should be of low distortion, which can be observed by the output of the Wheatstone bridge. A typical output waveform with 250 $\mu\varepsilon$ amplitude at 4.5 Hz with low distortion is shown in Fig. 7.

Metrol. Meas. Syst., Vol. 29 (2022), No. 4, pp. 751–762
DOI: 10.24425/mms.2022.143063

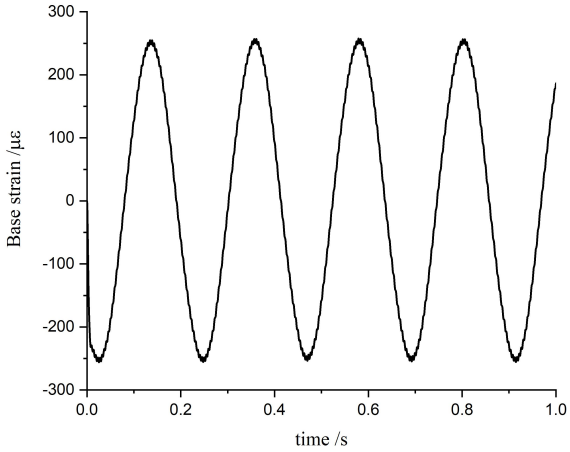

Fig. 7. Output waveform of the base strain.

3.2. Base strain sensitivity results

There are two SUTs to be calibrated, which can be marked as Sensor 1 and Sensor 2. Sensor 1 is the product of Brüel & Kjær, Denmark, and the type is 4384, which is used for general purpose vibration measurements, with the nominal sensitivity 1.0 pC/m·s^{-2}, and nominal base strain sensitivity 0.002 g/με. Sensor 2 is the product of Jiangsu Lianneng Co., Ltd, China, and the type is CA-YD-109A, which is mainly used to measure low-frequency vibration, with a nominal sensitivity of 1138.4 pC/m·s^{-2}, and nominal base strain sensitivity of 0.5 g/με. The base strain sensitivity of both Sensor 1 and Sensor 2 are calibrated with the traditional method. The amplitude linearity characteristics under 4.5 Hz and frequency response characteristics under 250 με of both SUTs are shown in Fig. 8.

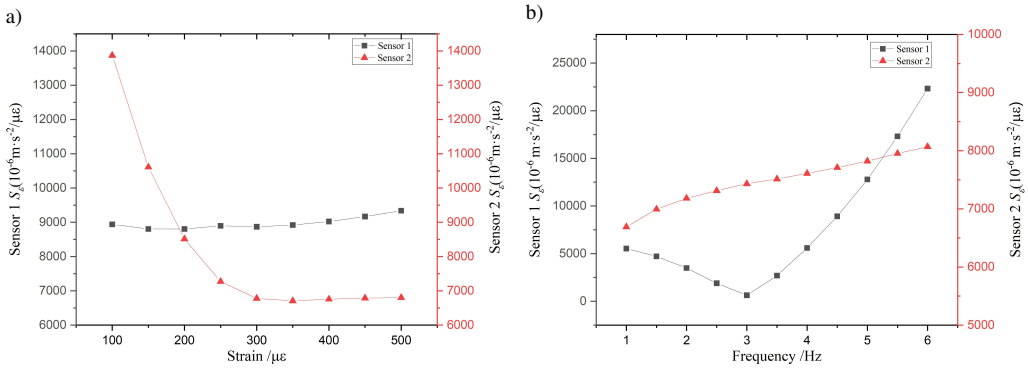

Fig. 8. Characteristics of base strain sensitivity from the SUT. Amplitude linearity (a) frequency response (b).

For the amplitude linearity characteristics of the two SUTs, the curve of Sensor 1 levels off in all experiments at approximately 0.009 m·s^{-2}/με. The curve of Sensor 2 shows a dramatic decrease when the base strain is smaller than 300 με, followed by a leveling off at approximately 0.0068 m·s^{-2}/με with a larger base strain applied. This difference between the two SUTs is

possible because of the different inner structures. Nevertheless, the maximum values are both smaller than the nominal values.

For the frequency response characteristics, when the excitation frequency is lower than 3 Hz, the base strain sensitivity of Sensor 1 declines, followed by a significant increase in the frequency band from 3 Hz to 6 Hz, although the waveform of the output oddly reverses at 3 Hz. The pattern of Sensor 2 always shows an increase over the whole frequency range. Moreover, similar to the results in amplitude linearity, the maximum values do not exceed the nominal values.

3.3. Uncertainty analysis

Considering that the components of the base strain sensitivity expressed in equation (14) are independent, according to the propagation law of uncertainty [20], the combined standard uncertainty of the base strain sensitivity can be derived as

$$u_{\mathrm{rel}}\left(S_{\varepsilon}\right)=\sqrt{u_{\mathrm{rel}}^{2}\left(a_{\varepsilon\,\mathrm{rms}}\right)+u_{\mathrm{rel}}^{2}\left(\varepsilon_{\mathrm{rms}}\right)}, \tag{15}$$

where $u_{\mathrm{rel}}\left(a_{\varepsilon\mathrm{rms}}\right)$ is the relative uncertainty in the RMS error output caused by the base strain and $u_{\mathrm{rel}}\left(\varepsilon_{rms}\right)$ is the relative uncertainty in the RMS base strain. The components of the B-class uncertainty are analyzed in detail as follows:

1. Uncertainty introduced by the measurement of $a_{\varepsilon\mathrm{rms}}$. According to equation (13) and the definition of relative standard uncertainty, $u_{\mathrm{rel}}\left(a_{\varepsilon\mathrm{rms}}\right)$ can be expressed as

$$u_{\mathrm{rel}}\left(a_{\varepsilon\,\mathrm{rms}}\right)=\frac{u\left(a_{\varepsilon\,\mathrm{rms}}\right)}{a_{\varepsilon\,\mathrm{rms}}}=\frac{\sqrt{u^{2}\left(a_{\mathrm{total,\,rms}}\right)+u^{2}\left(a_{\mathrm{base,\,rms}}\right)}}{\left(a_{\mathrm{total}}-a_{\mathrm{base}}\right)_{\mathrm{rms}}}, \tag{16}$$

where the uncertainties without an index are the standard uncertainties in the relative values.

According to the definition of the RMS, the denominator in equation (16) satisfies the relationship as

$$\left(a_{\mathrm{total}}-a_{\mathrm{base}}\right)_{\mathrm{rms}}^{2}=\frac{1}{T}\int_{0}^{T}\left(a_{\mathrm{total}}-a_{\mathrm{base}}\right)^{2}\mathrm{d}t=a_{\mathrm{total,\,rms}}^{2}+a_{\mathrm{base,\,rms}}^{2}-\frac{2}{T}\int_{0}^{T}a_{\mathrm{total}}\cdot a_{\mathrm{base}}\,\mathrm{d}t. \tag{17}$$

In equation (17), T is the sampling time. Then, the last item in (17) can be marked as $\zeta(t)$,

$$\zeta(t)=-\frac{2}{T}\int_{0}^{T}a_{\mathrm{total}}\cdot a_{\mathrm{base}}\,\mathrm{d}t. \tag{18}$$

Thus, according to equations (16) and (18), it can be obtained that

$$\begin{aligned}u_{\mathrm{rel}}^{2}\left(a_{\varepsilon\,\mathrm{rms}}\right)&=\frac{u^{2}\left(a_{\mathrm{total,\,rms}}\right)+u^{2}\left(a_{\mathrm{base,\,rms}}\right)}{a_{\mathrm{total,\,rms}}^{2}+a_{\mathrm{base,\,rms}}^{2}+\zeta(t)}\\&=\frac{u_{\mathrm{rel}}^{2}\left(a_{\mathrm{total,rms}}\right)+u_{\mathrm{rel}}^{2}\left(a_{\mathrm{base,rms}}\right)\cdot\left(\dfrac{a_{\mathrm{base,rms}}}{a_{\mathrm{all,rms}}}\right)^{2}}{1+\left(\dfrac{a_{\mathrm{base,rms}}}{a_{\mathrm{all,rms}}}\right)^{2}+\dfrac{\zeta(t)}{a_{\mathrm{all,rms}}^{2}}}.\end{aligned} \tag{19}$$

Metrol. Meas. Syst., Vol. 29 (2022), No. 4, pp. 751–762
DOI: 10.24425/mms.2022.143063

For $\dfrac{\zeta(t)}{a^2_{\text{all, rms}}}$, according to the Cauchy–Schwartz inequality, the following relationship

$$\left(\frac{\zeta(t)}{a^2_{\text{total, rms}}}\right)^2 = \frac{\dfrac{4}{T^2}\left(\displaystyle\int_0^T a_{\text{total}} \cdot a_{\text{base}}\,\mathrm{d}t\right)^2}{\dfrac{1}{T^2}\left(\displaystyle\int_0^T a^2_{\text{total}}\,\mathrm{d}t\right)^2} \le \frac{4\displaystyle\int_0^T a^2_{\text{total}}\,\mathrm{d}t \cdot \int_0^T a^2_{\text{base}}\,\mathrm{d}t}{\left(\displaystyle\int_0^T a^2_{\text{total}}\,\mathrm{d}t\right)^2} = \frac{4\displaystyle\int_0^T a^2_{\text{base}}\,\mathrm{d}t}{\displaystyle\int_0^T a^2_{\text{total}}\,\mathrm{d}t} \tag{20}$$

or

$$\left|\frac{\zeta(t)}{a^2_{\text{total, rms}}}\right| \le 2 \cdot \frac{a_{\text{base, rms}}}{a_{\text{total, rms}}} \tag{21}$$

would be satisfied.

Based on the collected data, the ratio on the right of inequality (21) is in the range of 0.01 to 0.1, which can be ignored. Then, equation (19) can be rewritten as

$$u^2_{\text{rel}}\left(a_{\varepsilon\,\text{rms}}\right) = \frac{u^2_{\text{rel}}\left(a_{\text{total, rms}}\right) + u^2_{\text{rel}}\left(a_{\text{base, rms}}\right) \cdot \left(\dfrac{a_{\text{base,rms}}}{a_{\text{total, rms}}}\right)^2}{1 + \left(\dfrac{a_{\text{base, rms}}}{a_{\text{total, rms}}}\right)^2}. \tag{22}$$

The RMS of the total response is always larger than that of the response caused by vibration, so

$$0 < \frac{a_{\text{base, rms}}}{a_{\text{total, rms}}} < 1. \tag{23}$$

According to equation (13),

$$u^2_{\text{rel}}\left(a_{\text{total, rms}}\right) = u^2_{\text{rel}}\left(u_{\text{total}}\right) + u^2_{\text{rel}}\left(S_{\text{base}}\right). \tag{24}$$

The maximum error of the u_{total} sampled by the controller is 0.1% and evenly distributed, so

$$u_{\text{rel}}(u_{\text{total}}) = \frac{0.1\%}{\sqrt{3}} = 0.058\%. \tag{25}$$

For S_{base}, the relative expanded uncertainty is given as 1% ($k = 2$). Thus,

$$u_{\text{rel}}(S_{\text{base}}) = 0.5\%. \tag{26}$$

Therefore,

$$u^2_{\text{rel}}\left(a_{\text{total, rms}}\right) = 2.533 \times 10^{-5}. \tag{27}$$

The maximum error of the $a_{\text{base}\,m}$ measured by the laser vibrometer is 0.5% and evenly distributed, so

$$u^2_{\text{rel}}\left(a_{\text{base, rms}}\right) = \left(\frac{0.5\%}{\sqrt{3}}\right)^2 = 8.352 \times 10^{-6}. \tag{28}$$

In summary,

$$u_{\text{rel}}\left(a_{\varepsilon\,\text{rms}}\right) = 0.503\%. \tag{29}$$

2. Uncertainty introduced by the measurement of base strain ε_{rms}. According to equation (8), in which the components of ε are independent, the relative standard uncertainty of the value can be expressed as

$$u_{\text{rel}}(\varepsilon_{\text{rms}}) = \sqrt{u_{\text{rel}}^2(u_{\text{BD}}) + u_{\text{rel}}^2(E) + u_{\text{rel}}^2(K)}\,. \tag{30}$$

The maximum error of u_{BD} sampled by the controller is 1%, and the maximum error of E in the bridge circuit is 0.05%, meeting the requirement of the stabilization of voltage, which should be limited within 0.1%. In addition, the maximum error of K of the strain gauges is given as 0.5% and evenly distributed, so

$$u_{\text{rel}}(\varepsilon_{\text{rms}}) = \sqrt{\left(\frac{0.1\%}{\sqrt{3}}\right)^2 + \left(\frac{0.05\%}{\sqrt{3}}\right)^2 + \left(\frac{0.5\%}{\sqrt{3}}\right)^2} = 0.297\%. \tag{31}$$

In summary, the relative standard uncertainty of the calibrated base strain sensitivity can be expressed as

$$u_{\text{rel}}\,(S_\varepsilon) = \sqrt{u_{\text{rel}}^2\,(a_{\varepsilon\,\text{rms}}) + u_{\text{rel}}^2\,(\varepsilon_{\text{rms}})} = 0.584\%. \tag{32}$$

The coverage factor is two, and the uncertainty ($k = 2$) of the base strain sensitivity is less than 2%.

4. Conclusions

By driving a cantilever beam with an electromagnetic excitor, the base strain can be generated harmonically between 1 Hz and 6 Hz, from 50 $\mu\varepsilon$ up to 500 $\mu\varepsilon$, and both of the frequency and the strain can be adjusted continuously. The generated strain with low distortion can be measured with a Wheatstone bridge circuit. The adverse vibration introduced to the SUT can be dismissed by a particular compensating method. The uncertainty in the calibration results is less than 2% ($k = 2$). With this novel method, a more accurate and efficient calibration can be achieved which suffers the least from manual interference.

In the future researches, there are two aspects to be improved and explored. Firstly, to prevent the vibration being introduced to the base of the sensor, a new mechanical structure can be designed in which the mounting point of the sensor is always static and only the strain will be applied on the base; secondly, the mechanism of base strain sensitivity can be deduced and simulated, which makes it possible to reveal the reason why the piezoelectric material causes spurious signals when bending strain is applied.

Acknowledgements

This work was supported in part by the National Key R&D Program of China (Grant No. 2019YFC 1509503), in part by the National Science and Technology Major Project (Grant No. 2016ZX05008008), and in part by the National Natural Science Foundation of China (Grant No. 51875520).

References

[1] Yaghootkar, B., Azimi, S., & Bahreyni. B. (2017). A high-performance piezoelectric vibration sensor. *IEEE Sensors Journal, 17*(13), 4005–4012. https://doi.org/10.1109/JSEN.2017.2707063

Metrol. Meas. Syst., Vol. 29 (2022), No. 4, pp. 751–762
DOI: 10.24425/mms.2022.143063

[2] Xiaoning, J., Kyungrim, K., Shujun, Z., Joseph J., & Giovanni, S. (2014). High-temperature piezoelectric sensing. *Sensors*, *14*(1), 144–169. https://doi.org/10.3390/s140100144

[3] Roger, de R., Jens, O. G., & Patrick R. S. (1999). Fabrication and characterization of a piezoelectric accelerometer. *Journal of Micromechanics and Microengineering, 9*, 123–126. https://doi.org/10.1088/0960-1317/9/2/005

[4] Kim, K., Zhang, S., Salazar, G., & Jiang, X. (2012). Design, fabrication and characterization of high temperature piezoelectric vibration sensor using YCOB crystals. *Sensors and Actuators A: Physical*, 178, 40–48. https://doi.org/10.1016/j.sna.2012.02.003

[5] Shujung, Z., Xiaoning, J., Michael, L., Paul, Moses., & Thomas, R. S. (2010). Piezoelectric accelerometer for ultrahigh temperature application. *Applied Physics Letters, 96*(1),013506. https://doi.org/10.1063/1.3290251

[6] Kong, L. F., Yu, F. P., Qin, L. F., Cheng, X. F., & Zhao, X. (2017, October). Performance improvement of CTGS and YCOB crystals for high temperature piezoelectric accelerometer applications. In *2017 Symposium on Piezoelectricity, Acoustic Waves, and Device Applications (SPAWDA)* (pp. 117–120). IEEE. https://doi.org/10.1109/SPAWDA.2017.8340301

[7] Flanagan, P., & Lekki, J. (2001, November). A self-diagnostic system for the M6 accelerometer. In *37th Joint Propulsion Conference and Exhibit* (pp. 3318). https://doi.org/10.2514/6.2001-3318

[8] Korobiichuk, I., Bezvesilna, O., Kachniarz, M., Koshovyj, M., & Kvasnikov, V. (2017, May). Methods and ways of piezoelectric accelerometers fastening on the objects of research. In *Proceedings of the International Conference on Oxide Materials for Electronic Engineering* (Vol. 59). http://doi.org/10.12693/APhysPolA.133.1112

[9] Von Martens, H. J. (1999). Current state and trends of ensuring traceability for vibration and shock measurements. *Metrologia, 36*(4), 357–373. https://doi.org/10.1088/0026-1394/36/4/16

[10] Usuda, T., Ohta, A., Ishigami, T., Fuchiwaki, O., Misaki, D., Aoyama, H., & Sato, S. (2004). The current progress of measurement standards for vibration in NMIJ/AIST. In *Proceedings of the Sixth International Conference on Vibration Measurements by Laser Techniques: Advances And applications* (pp. 30–38). SPIE. https://doi.org/10.1117/12.579527

[11] Daniel, S., & Christian, H. (2020). Primary accelerometer calibration by scanning laser Doppler vibrometry. *Measurement Science and Technology, 31*(6), 065006. https://doi.org/10.1088/1361-6501/ab66da

[12] Jitendra, C., Vijayalakshmi, V., Sridhar, B. (2018). Revamping an Accelerometer calibration System-A "Better-than-New" Approach. In *2018 5th IEEE Uttar Pradesh Section International Conference on Electrical, Electronics and Computer Engineering (UPCON)*. Gorakhpur, India, 2018, 1–4. https://doi.org/10.1109/UPCON.2018.8596933

[13] Tian, B., Liu, H., Yang, N., Zhao, Y., & Jiang, Z. (2016). Design of a piezoelectric accelerometer with high sensitivity and low transverse effect. *Sensors*, *16*(10), 1587. https://doi.org/10.3390%2Fs16101587

[14] International Organization for Standardization. (1987). *Standard:5347-0: Methods for the calibration of vibration and shock pick-ups-part 0: Basic concepts*. https://www.iso.org/standard/11345.html

[15] Usuda, T., Weißenborn, C., & Von Martens, H. J. (2004). Theoretical and experimental investigation of transverse sensitivity of accelerometers under multiaxial excitation. *Measurement Science and Technology, 15*(5), 896–904. https://doi.org/10.1088/0957-0233/15/5/017

[16] Benjamin, S., Jingxiang, S., Ron-Marco, F., Florian, N., Simon, F., Fabian, L., & Franz, F. (2021). Influence of the piezoelectric material on the signal and noise of magnetoelectric magnetic field sensors based on the delta-E effect. *APL Materials*, *9*, 031108. https://doi.org/10.1063/5.0042448

[17] Andrea, P., Fabrizio, M. & Alessandro, S. (2020). Traceability of digital 3-axis MEMS accelerometer: simultaneous determination of main and transverse sensitivities in the frequency domain. *Metrologia, 57*(3), 035013. https://doi.org/10.1088/1681-7575/ab79be

[18] Du, Y., Gao, G., & Li, T. (2018). A novel method for testing accelerometer transverse sensitivity. *Review of Scientific Instruments*, *89*(12), 125003. https://doi.org/10.1063/1.5034191

[19] International Organization for Standardization. (1987). *Standard:5347-13: Methods for the calibration of vibration and shock pick-ups-part 13: Testing of base strain sensitivity*. International Organization for Standardization. https://www.iso.org/standard/11359.html

[20] International Organization for Standardization. (2008). *JCGM 100: Evaluation of measurement data-guide to the expression of uncertainty in measurement*. International Organization for Standardization. https://ncc.nesdis.noaa.gov/documents/documentation/JCGM_100_2008_E.pdf

Chuwei Ye received his M.Sc. and B.Sc. from Zhejiang University, China in 2020 and 2017, respectively. He is currently pursuing his Ph.D. degree at Michigan State University, Michigan, the United States. His research interests include vibration sensor calibration systems, and dynamical strain and stress measurement.